Nanoscale

Accepted Manuscript

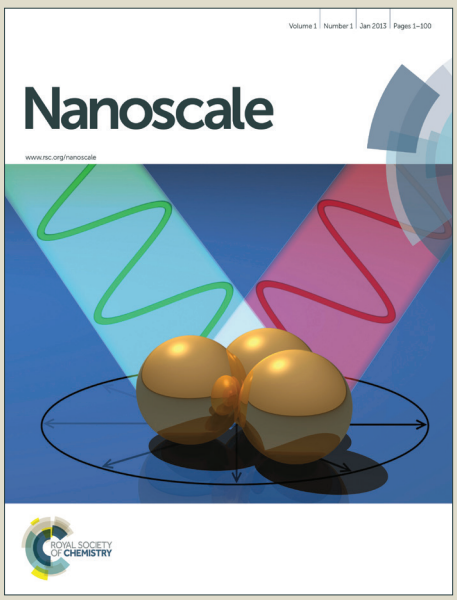

ROYAL SOCIETY OF CHEMISTRY

www.rsc.org/nanoscale

Nanoscale

RSCPublishing

Paper

Room-temperature self-powered ethanol sensing of Pd/ZnO nanoarray nanogenerator driven by human finger movement

Cite this: DOI: 10.1039/x0xx00000x

Received 00th January 2012,
Accepted 00th January 2012

DOI: 10.1039/x0xx00000x

www.rsc.org/

Yujie Lin[a], Ping Deng[a], Yuxin Nie[a], Yuefeng Hu[a], Lili Xing[a], Yan Zhang[*b,c] and Xinyu Xue[*a,b]

Flexible room-temperature self-powered active ethanol sensor has been realized from Pd/ZnO nanoarray nanogenerator. Pd nanoparticles are uniformly loaded on the whole surface of ZnO nanowire arrays by a simple hydrothermal method. The piezoelectric output of Pd/ZnO nanowire arrays can act as both the power source of the device and the room-temperature ethanol sensing signal. Upon exposure to 800 ppm ethanol gas at room temperature, the piezoelectric output voltage decreased from 5.2 V (in air) to 2.5 V. Such a room-temperature self-powered ethanol sensing behavior can be attributed to the catalytic effect of Pd, the Schottky barrier at Pd/ZnO interface, and the piezotronics effect of ZnO nanowires. Moreover, this flexible device can be driven by tiny mechanic energy in our environment, such as human finger movement. The present results can stimulate a research trend on designing new material system and device structure in self-powered ethanol sensing at room temperature.

Introduction

With the rapid development of functional nanodevices, such as gas sensors, biosensors and UV detector, seeking of portable, small-size and sustainable power sources for driving these nanodevices is becoming increasingly important. In the past several years, self-powered system that integrates energy generators and functional devices has been proposed,[1,2] aiming at harvesting energy from the environment to power the functional micro/nano-systems, such as pH sensors, UV detectors, liquid crystal displays, etc.[3] Most recently, a new type of self-powered nanosystem, named as an active sensor has been demonstrated by treating the output piezoelectric signal from nanogenerators as either a power source or sensing signal in response to the change in environment, such as ambient wind velocity detectors, automobile speedometers, gas sensors and magnetic sensors.[4,5] Gas sensors have attracted world-wide attention due to their significant applications in industrial production, public transportation and people's daily life.[6-9] In the past several decades, one-dimensional (1D) metal oxide nanostructures, such as ZnO, SnO_2 and In_2O_3 nanowires/rods,[10-13] have greatly enhanced the sensitivity of gas sensors resulting from their high surface-to-volume ratio. Among them, ZnO 1D nanostructures have been extensively investigated due to their high conductivity, good stability and biological friendliness.[14-16] Upon exposure to reducing gas, such as ethanol, the reaction between ethanol molecules and oxygen ions on the surface of ZnO nanostructures releases free electrons flowing back to the conduction band and decreasing the depletion width, leading to a great increase of conductivity of ZnO nanostructures (N-type semiconductor).[17] On the other hand, the high work temperature (200-300 ℃) required for the chemical reaction between ethanol and oxygen ion restrains the practical applications of the ZnO-based gas sensor, such as explosive and flammable environment. In our previous work, by coupling the piezoelectric and gas sensing characteristics of ZnO nanowire (NW) arrays, an unpackaged ZnO NW piezo-nanogenerator (NG) as a self-powered active gas sensor that can detect H_2S (with strong reducibility) at room temperature has been firstly demonstrated.[4] However, self-powered detecting low reducing gas, such as ethanol vapor, remains a challenge. Noble metal decoration on 1D metal oxide nanostructures, such as Pd, Au and Pt,[18-20] has been confirmed to have potentials on lowering down the work temperature of traditional ethanol sensors. Thus, if the noble metal decoration can be introduced into self-powered active gas sensing, then room-temperature ethanol sensing can probably be realized.

In this paper, ZnO NW arrays are uniformly loaded with Pd nanoparticles, and room-temperature ethanol sensing has been realized from Pd/ZnO self-powered active gas sensor. The piezoelectric output of Pd/ZnO nanoarray NG can act not only as a power source, but also as a response signal to ethanol at room temperature. Upon exposure to 800 ppm ethanol gas, the piezoelectric output of the device decreases from 0.52 V (in air) to 0.25 V. Such a room-temperature ethanol sensing can be attributed to the catalytic properties of Pd nanoparticles, the Schottky barriers at Pd/ZnO interfaces, and the coupling of piezoelectric and semiconducting properties of ZnO (piezotronics effect). Our study can stimulate a research trend on designing new material system and device structures for room-temperature self-powered active gas sensors.

Experimental

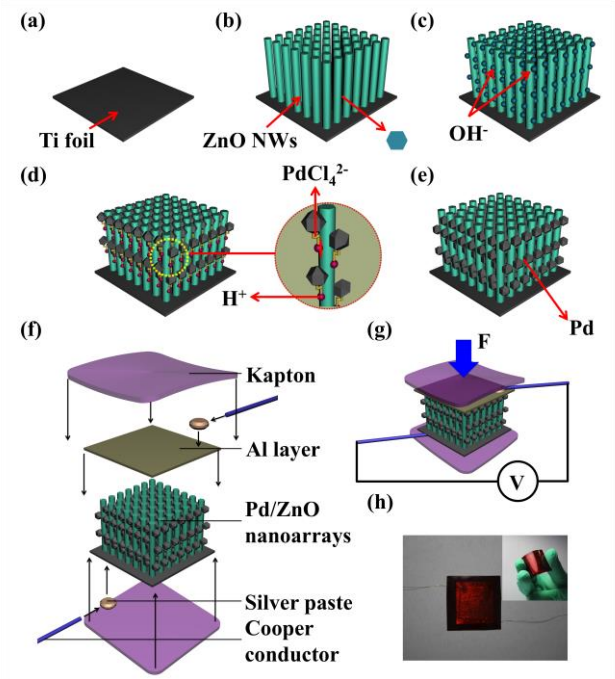

Figure 1. Fabrication process of the self-powered active gas sensor based on Pd/ZnO nanoarrays. (a) A pre-cleaned Ti foil is used as the substrate. (b) Vertically-aligned ZnO NW arrays are grown on Ti foil. (c) Free hydroxyl groups (provided by NaOH) are attached to the surface of ZnO NWs. (d) The attached hydroxyl groups are protonated and conjugate with $PdCl_4^{2-}$ ions via electrostatic attraction. (e) $PdCl_4^{2-}$ ions are reduced, and Pd is nucleated and located on the surface of ZnO NWs. (f) Schematic diagram showing the assembling of self-powered active ethanol sensor. (g) Schematic diagram showing the final device structures. The piezoelectric output voltage under constant compressive strain is dependent on the concentration of ethanol atmosphere. (h) The optical image of the device, showing that it can be easily bended by human fingers.

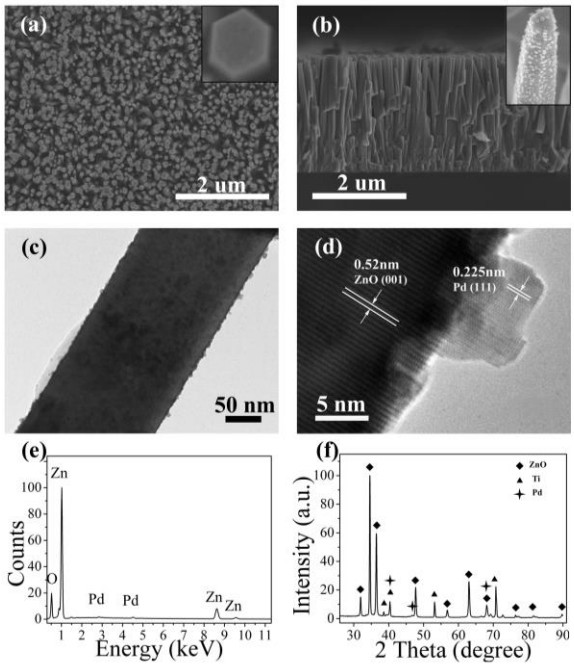

Figure 2. (a) SEM image of Pd/ZnO NW arrays in a top view. The inset is an enlarged view of the tip of Pd/ZnO NW. (b) SEM image of Pd/ZnO NW arrays in a side view. The inset is an enlarged view of one single Pd/ZnO NW, showing that Pd nanoparticles are uniformly loaded on the whole surface of ZnO NW. (c) TEM image of one single Pd/ZnO NW. ZnO NW is uniformly covered with Pd nanoparticles. (d) HRTEM image of Pd/ZnO interface. (e) EDS spectrum of Pd/ZnO NW arrays. (f) XRD pattern of Pd/ZnO NW arrays on Ti substrate.

Figure 1 shows a brief fabrication process and the structure of the self-powered active gas sensor based on Pd/ZnO NW arrays. Prior to the growth of ZnO NW arrays, a piece of Ti foil as the substrate is cleaned with water/alcohol and dried at 60 ℃, as shown in Figure 1a. ZnO NW arrays are then vertically grown on the Ti foil by a simple hydrothermal method (Figure 1b). 0.52g of $Zn(NO_3)_2$ $6H_2O$ were dissolved in 50 ml of distilled water. After magnetically stirring for 10 min, 2 ml of NH_3 H_2O was added into the solution drop by drop. The Ti substrate was immersed into the solution. It was then sealed and maintained at 70 ℃ for 24 h. After cooling down to room temperature, the Ti substrate coated with ZnO NW arrays was removed from the solution, washed with deionized water, and dried at 60 ℃. Then Pd nanoparticles were uniformly loaded on the surface of ZnO NW arrays by a hydrothermal method (Figure 1c, d and e). 70 μl of $PdCl_2$ aqueous solution (0.057 M, and containing small amount of HCl) was added into 40 ml NaOH aqueous solution (pH value=9) drop by drop. The mixed solution was transferred into a 50 ml Teflon-lined stainless steel autoclave, and the Ti substrate coated with ZnO NW arrays was immersed into the solution. It was then sealed and maintained at 180 ℃ for 0.5h. At this stage, free hydroxyl groups (provided by NaOH) are attached to the surface of ZnO nanowire, as shown in Figure 1c. The attached hydroxyl groups are protonated and conjugate with $PdCl_4^{2-}$ ions via electrostatic attraction,[18] as shown in Figure 1d. $PdCl_4^{2-}$ ions are then reduced, and Pd is nucleated and located on the surface of ZnO nanowires,[18] as shown in Figure 1e. After cooling down to room temperature, the substrate was removed from the solution, washed with water/alcohol and dried at 60 ℃.

Figure 1f shows the assembling of the self-powered active gas sensor. The Ti foil acts as both the substrate for Pd/ZnO NW arrays and a conductive electrode. A piece of Al foil (thickness=0.05 mm) positioned on the top of Pd/ZnO NW arrays acts as the counter electrode. Two cooper conducting leads were glued on the two electrodes with silver paste, respectively. The device was finally sealed in two pieces of Kapton board as the frame. As shown in Figure 1g, the final device was connected to an outside circuit (low-noise preamplifier; Model SR560, Stanford Research Systems), which independently monitors the change of piezoelectric output voltage upon exposure to ethanol gas. An optical image of the device is shown in figure 1h, indicating that the device is very flexible and can be easily bended by human finger.

Results and discussion

Figure 2a is a typical scanning electron microscopy (SEM) image of Pd/ZnO nanoarrays on the top-view, revealing a consistent growth direction. The inset of Figure 2a is an enlarged view of the tip of Pd/ZnO NW, indicating the typical hexagonal cross-sectional shape of Pd/ZnO NW.[21,22] The average diameter of Pd/ZnO nanowires is about 200 nm. The side view of Pd/ZnO NW arrays in Figure 2b reveals that the NWs are vertically aligned on the substrate, and the average length of the nanoarrays is about 2.5 μm. The fracture of the

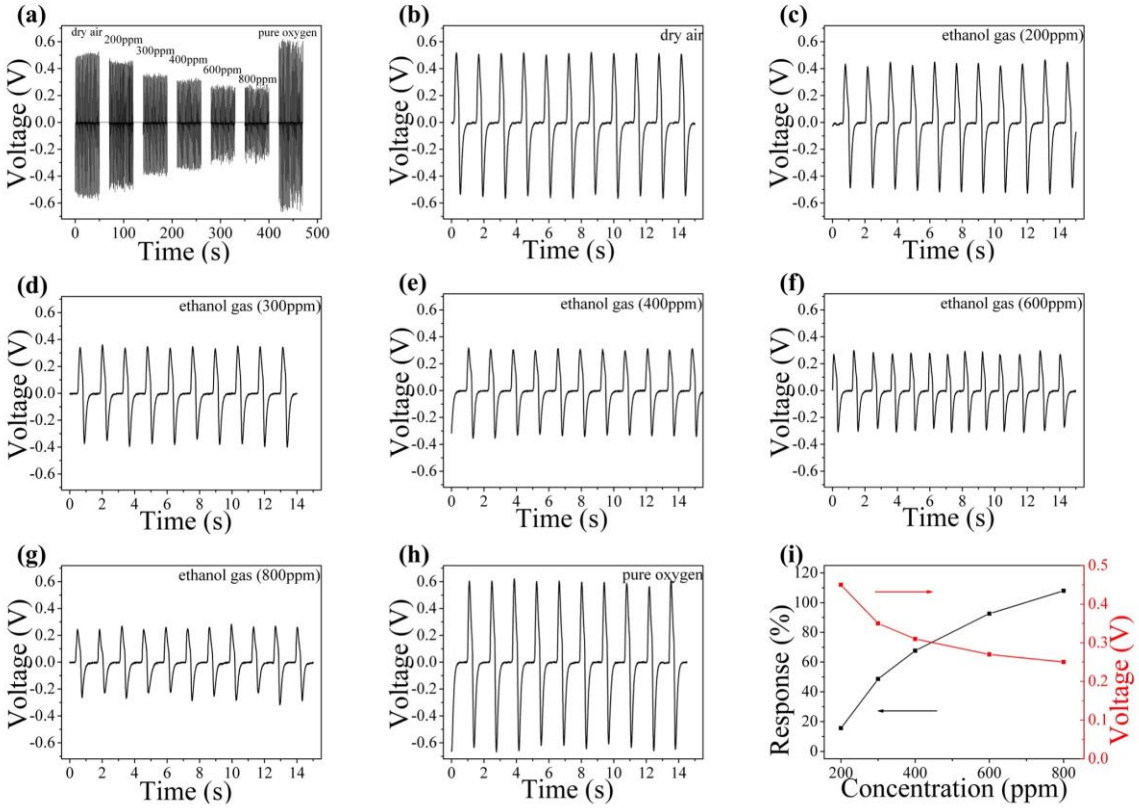

Figure 3. (a) The piezoelectric output voltage of the device at room temperature upon exposure to dry air, ethanol gas and pure oxygen under the same applied strain (0.012%). (b), (c), (d), (e), (f), (g) and (h) are enlarged views of the piezoelectric output in dry air, 200, 300, 400, 600, 800 ppm ethanol gas and pure oxygen, respectively. (i) The dependence of the response and piezo-voltage on the concentration of ethanol gas.

NWs arises from the break-in operation on the sample for SEM observation. The inset of Figure 2b is an enlarged view of one single Pd/ZnO NW, confirming that ZnO NW is uniformly coated with Pd nanoparticles. Transmission electron microscopy (TEM) image of Pd/ZnO NW (Figure 2c) further confirms that ZnO NW is uniformly loaded with Pd nanoparticles. It can also be seen that the average diameter of Pd nanoparticles is about 5 nm. Figure 2d is a high-resolution transmission electron microscopy (HRTEM) image of Pd/ZnO interface. Both ZnO and Pd are of single-crystal structures. The interplanar distance of 0.225 nm corresponds to (111) plane of Pd. The interplaner distance of 0.52 nm corresponds to the (001) plane of ZnO. Figure 2e is energy dispersive spectroscopy (EDS) spectrum of Pd/ZnO nanoarrays, showing the existence of three elements (O, Zn and Pd) in this selected region. Similar EDS results have been obtained at 10 other different areas, which further confirm that Pd nanoparticles are uniformly distributed in the whole system. Figure 2f is an X-ray diffraction (XRD) pattern of Pd/ZnO nanoarrays. The peaks marked with diamond can be indexed to ZnO (JCPDS file no. 36-1451); the peak marked with asterisk can be indexed to Pd crystal (JCPDS file no. 65-6174); and the peak marked with trigon can be indexed to Ti foil substrate (JCPDS file no. 44-1294). No sharp peaks can be indexed to other impurities, indicating a high crystal quality of Pd/ZnO. Figure 3a shows the piezoelectric output voltage of the Pd/ZnO nanoarray NG at room temperature upon exposure to dry air, ethanol gas and pure oxygen under the same applied strain (34N, 0.012%, 0.45 Hz). The measurement is not continuous, in which the exposure time is long enough for ethanol adsorption. All the measurements are conducted under the pressure of 1.01×10^5 Pa. Figure 3b-h are enlarged views of the piezoelectric output in dry air, 200, 300, 400, 600, 800 ppm ethanol gas and pure oxygen. The piezoelectric voltage in dry air is about 0.52 V. Upon exposure to 200, 300, 400, 600 and 800 ppm ethanol gas, the piezoelectric output voltage of the device is about 0.45, 0.35, 0.31, 0.27 and 0.25 V, respectively. When the device is exposed to pure oxygen, the piezoelectric output is about 0.60 V. The piezoelectric output of the device is dependent on the outside atmosphere, and the piezoelectric output decreases with increasing concentration of ethanol gas. Similar to the traditional definition of sensitivity of gas sensors ($S\% = \frac{|R_a - R_g|}{R_g}\times100\%$,[23] where R_a and R_g represent the resistance of the sensor in dry air and in the test gas, respectively), the response of the self-powered active ethanol sensor can be simply defined as follows:

$$Response = \frac{|V_a - V_g|}{V_g}\times100\% \quad (1)$$

, where V_a represents the piezoelectric output voltage of the device in dry and V_g represents the piezoelectric output voltage of the device in test gas. As shown in figure 3i, the response of the device against 200, 300, 400, 600 and 800 ppm ethanol gas is 15.6%, 48.6%, 67.7%, 92.6% and 108.0%. Highly-sensitive

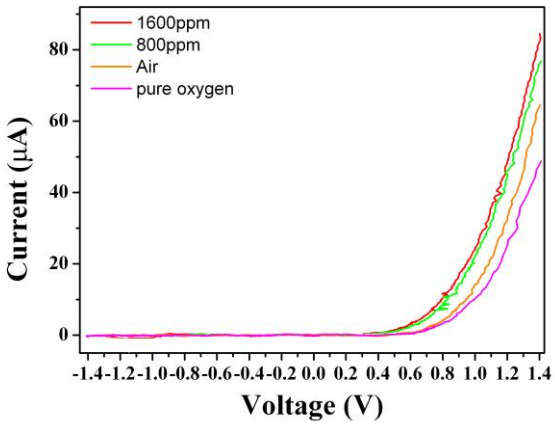

Figure 4. The *I-V* curves of one device in dry air, pure oxygen, 800 ppm and 1600 ppm ethanol gas without deformation at room temperature.

room-temperature ethanol sensing has been obtained from Pd/ZnO nanoarray self-powered active gas sensor. These experimental results suggest that the room-temperature self-powered ethanol sensing of Pd/ZnO nanoarray NG has potential applications at the industrial level.

Such a piezo-gas sensing behavior can be attributed the coupling of the piezotronics effect of ZnO and the gas sensing properties of Pd/ZnO. Firstly, it has been confirmed that the piezoelectric effect of ZnO nanowires can be influenced by the free-carriers within them, and this phenomenon has been named as "piezotronics effect.[2,5,24-30] As the c-axis of ZnO NW (n-type semiconductor arising from the point defects within it) is under externally applied deformation[31], a piezoelectric field can be created on the surface that can not only drive the electrons in the external circuit flowing forward and back (the output of NG), but also make the free electrons on the surface of ZnO NWs migrate and partially screen this piezoelectric field (piezotronics effect).[32,33] Previous theoretical and experimental works also confirm that the change in free-carrier density can affect the piezoelectric output of ZnO NW NG.[4,34,35] Secondly, it is well known that the free-carrier density of ZnO NWs can be affected by oxidizing or reducing gas adsorbed on the surface, which is the traditional gas sensing mechanism of ZnO NWs.[18,19] Such a change of free-carrier density of the Pd/ZnO NWs can be directly demonstrated by the measurement of conductance. Figure 4 shows the I–V curves of one device in different concentration of ethanol without deformation at room temperature. There is a typical metal–semiconductor–metal (M–S–M) structure in our device. The nonlinear I–V characteristic is caused by the asymmetric barrier heights formed between Pd/ZnO NWs and two metal electrodes. With the increasing ethanol concentration, the conductance of Pd/ZnO NWs increases, which strongly and directly confirm the increase of carrier density in ZnO NWs. Here, the decoration of Pd nanoparticles improves the gas sensing performance due to the catalysis effect of Pd and the Schottky barrier between Pd and ZnO. For using as a typical ethanol sensor with normal work mode, the resistance of the sensor changes at different concentrations of the test gas. The ethanol will affect the surface carrier density (surface depletion layer) of NWs by the catalytic reaction. However, the response is low without coupling piezotronics effect at room temperature. Comparing the new work mode (piezo-gas sensing), the response is significantly enhanced under the new coupling work mechanism. For the traditional gas sensing, the change of surface depletion contributes a small portion of total resistance change (the internal resistance does not change), especially at room temperature. For the piezo-gas sensing, the piezoelectric effect is entirely influenced by the surface charge screening, thus it is very sensitive to the surface charge change induced by test gas adsorption. Thirdly, it can be scientifically deduced that the piezoelectric output of Pd/ZnO NWs can be influenced by the ethanol adsorption on the surface. The detailed working mechanism is discussed below.

Figure 5 shows the work mechanism of Pd/ZnO nanoarray self-powered active ethanol sensor. When the device is in dry air without any applied deformation (Figure 5a), the device is in natural state without any piezoelectric output. Since work function of ZnO (~4.5 eV) is smaller than that of Pd (5.12 eV),[36-38] the electrons flow from ZnO to Pd, establishing Schottky barrier at Pd/ZnO interface. The Schottky barrier leads to the depletion of electrons on ZnO NW surface. At the same time, Pd can also provide a chemical mechanism for the depletion of electrons on ZnO NW surface,[39] as shown in the inset of Figure 5a. Pd nanoparticles catalytically activate the adsorption and dissociation of molecular oxygen on the surface of ZnO NWs, in which oxygen molecules capture free electrons from ZnO NWs and form oxygen ions (O_2^-). During this process, both the quantity of oxygen that can repopulate surface vacancies and the rate at which this repopulation occurs are greatly increased by Pd catalysis (Pd is a far better oxygen dissociation catalyst than ZnO), which result in a greater/faster withdrawal of electrons from ZnO NWs even at room temperature (spillover effect, process [1] in Figure 5a).[39] According to the previous research, the size of spillover zone (Rsz) for oxygen is several tenths of nanometers.[39] In our case, the spillover zones can overlap the entire surface of ZnO NWs because Pd nanoparticles are uniformly coated on the whole surface of ZnO NWs and the distribution density is high enough (as shown in Figure 2c). And oxygen molecules can reside briefly on ZnO NW and diffuse to catalytic Pd nanoparticle before it has an opportunity to desorb, and the capture radius is R_{CR} (back-spillover effect, process [2] in Figure 5a).[39] Thus due to the physical/catalytic properties of Pd nanoparticles, the electron depletion on ZnO NW surface is very strong in air. When the device in air is under a compressive strain (Figure 5b), a piezoelectric field is created along Pd/ZnO NW arrays.[40] As the surface electron density in ZnO NW is very low in air, the screen effect on the piezoelectric output is greatly decreased, which enhance the piezoelectric output. In pure oxygen, the amount of oxygen molecules is larger than that in air, and the piezoelectric output is higher.

When the device is exposed to ethanol gas (Figure 5c), the

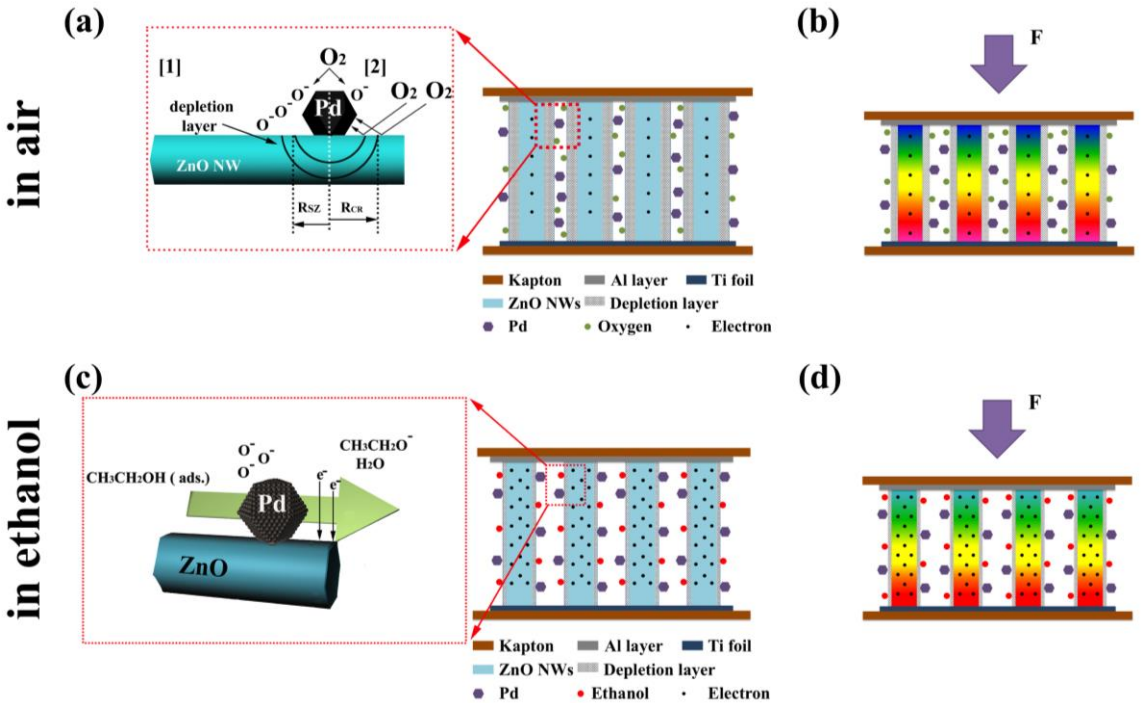

Figure 5. The working mechanism of Pd/ZnO self-powered active ethanol sensor driven by compressive strain. (a) Schematic illustration of the charge-carrier density and depletion layer in Pd/ZnO NW arrays without compression in dry air. The inset is schematic illustration of two major chemisorption processes of oxygen ions near Pd/ZnO interface. (b) Schematic illustration of the piezoelectric output of Pd/ZnO NW arrays in air under mechanical deformation. (c) Schematic illustration of the charge-carrier density and depletion layer in Pd/ZnO NW arrays without compression in ethanol gas. The inset shows the chemical reaction between ethanol and oxygen ions with the assistance of Pd catalysis. (d) Schematic illustration of the piezoelectric output of Pd/ZnO NW arrays in ethanol gas under mechanical deformation.

ethanol gas can undergo a reversible dissociation with the assistance of Pd catalysis as follows:[41,42]

$$CH_3CH_2OH\,(\text{gas}) \overset{Pd}{\leftrightarrow} CH_3CH_2OH\,(\text{ads.}) \quad (2)$$

$$CH_3CH_2OH\,(\text{ads.}) \overset{Pd}{\leftrightarrow} CH_3CH_2O\,(\text{ads.}) + H\,(\text{ads.}) \quad (3)$$

At room temperature, catalytic activity of Pd nanoparticles can greatly accelerate the reactions. Further Pd-assistant reaction between absorbed hydrogen and oxygen ions on the surface of Pd/ZnO nanoarrays can release electrons flowing back to ZnO NWs as follows:[41,42]

$$4H\,(\text{ads.}) + O_2^-\,(\text{ads.}) \overset{Pd}{\leftrightarrow} 2H_2O\,(\text{gas}) + e^- \quad (4)$$

The surface electron density in ZnO NWs is greatly increased.[41,42] When the device in ethanol is under a compressive strain (Figure 5d), the higher surface electron density in ZnO NWs results in a stronger screening effect on the piezoelectric output, and the piezoelectric output in ethanol gas is much lower than that in air.

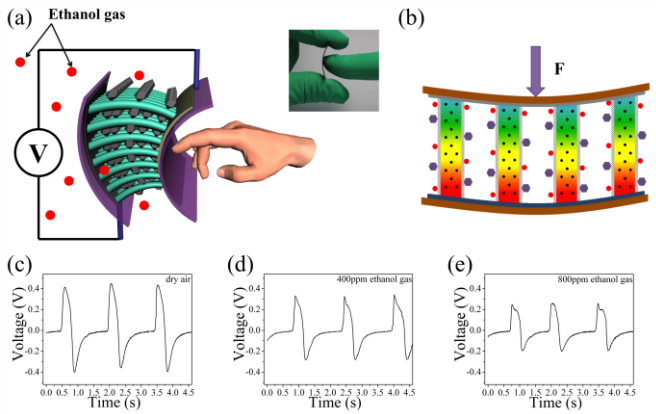

Figure 6. (a) Schematic diagram showing that the flexible self-powered active ethanol sensor can be driven by human finger movement. (b) Schematic illustration of the piezoelectric output of the flexible device in ethanol gas. Figure (c), (d) and (e) are experimental piezoelectric output driven by human finger movement in air, 400 and 800 ppm ethanol gas, respectively.

Flexible device structure of Pd/ZnO nanoarray NG as self-powered active ethanol sensor can effectively convert tiny mechanical energy into electricity signal, such as human finger movement, as shown in Figure 6a. Human finger pushing can provide compressive force on the device, and generate piezoelectric output, as schematically shown in Figure 6b. Figure 6c, d and e show the piezoelectric output of the device with human finger pushing in dry air, 400 and 800 ppm ethanol gas, respectively. The piezoelectric output voltage is about 0.43V, 0.35V and 0.25V, respectively. This result demonstrates the feasible applications of Pd/ZnO nanoarray self-powered active ethanol sensor in our living environment.

Conclusions

In summary, room-temperature ethanol sensing was obtained from Pd/ZnO nanoarray NG as self-powered active gas sensor. The piezoelectric output generated by Pd/ZnO nanoarray NG acted not only as a power source, but also a response signal to

ethanol at room temperature. The chemical and physical properties of Pd greatly improved the ethanol sensing performance at room temperature. Moreover, the flexible device structures driven by human finger movement was demonstrated. This research could stimulate a research trend on room-temperature self-powered active gas sensors.

Acknowledgements

This work was supported by the National Science Foundation of China (51102041 and 11104025), the Fundamental Research Funds for the Central Universities (N120205001, N120405010 and lzujbky-2013-35), program for New Century Excellent Talents in University (NCET-13-0112)

Notes and references

[a] College of Sciences, Northeastern University, Shenyang 110004, China. E-mail: xuexinyu@mail.neu.edu.cn

[b] Beijing Institute of Nanoenergy and Nanosystems, Chinese Academy of Sciences, Beijing 100000, China.

[c] Institute of Theoretical Physics, Lanzhou University, Lanzhou 730000, China. E-mail: yzhang@binn.cas.cn

1 X. D. Wang, J. Song, J. Liu and Z. L. Wang, *Science*, 2007, 361(5821), 102-105.
2 X. D. Wang, X. Wang, J. Zhou, J. Song, J. Liu, N. Xu and Z. L. Wang, *Nano Lett.*, 2006, 6(12), 2768-2772.
3 Z. L. Wang, Nano Today, 2010, 5(6), 512-514.
4 X. Xue, Y. Nie, B. He, L. Xing, Y. Zhang and Z. L. Wang, *Nanotechnology*, 2013, 24, 225501.
5 Y. F. Gao, Z. L. Wang, *Nano Lett.*, 2009, 9(3), 1103-1110.
6 C. Hagleitner, A. Hierlemann, D. Lange, A. Kummer, N. Kerness, O. Brand and H. Baltes, *Nature*, 2001, 414, 293-296.
7 J. Kong, *Science*, 2000, 287, 622-625.
8 E. Comini, G. Faglia, G. Sberveglieri, Z. Pan and Z. L. Wang, *Appl. Phys. Lett.*, 2002, 81, 1869.
9 Y. Chen, C. Zhu, L. Wang, P. Gao, M. Cao and X. Shi, *Nanotechnology*, 2009, 20, 045502.
10 Q. Wan, Q. H. Li, Y. J. Chen, T. H. Wang, X. L. He, J. P. Li and C. L. Lin, *Appl. Phys. Lett.*, 2004, 84, 3654.
11 Y. J. Chen, L. Nie, X. Y. Xue, Y. G. Wang and T. H. Wang, *Appl. Phys. Lett.*, 2006, 88, 083105.
12 P. Feng, X. Y. Xue, Y. G. Liu and T. H. Wang, *Appl. Phys. Lett.*, 2006, 89, 243514.
13 L. Wang, H. Dou, Z. Lou and T. Zhang, *Nanoscale*, 2013, 5, 2686-2691.
14 Z. L. Wang, *Journal of Physics: Condensed Matter*, 2004, 16, R829.
15 P. Yang, H. Yan, S. Mao, R. Russo, J. Johnson, R. Saykally, N. Morris, J. Pham, R. He and H. J. Choi, *Adv. Funct. Mater.*, 2002, 12, 323.
16 X. Wang, X. Wang, C. J. Summers and Z. L. Wang, *Nano Lett.*, 2004, 4, 423-426.
17 T. J. Hsueh, C. L. Hsu, S. J. Chang and I. C. Chen, *Sensors Actuat. B-Chem.*, 2007, 126, 473-477.
18 L. L. Xing, C. H. Ma, Z. H. Chen, Y. J. Chen and X. Y. Xue, *Nanotechnology*, 2011, 22, 215501.
19 N. Hongsith, C. Viriyaworasakul, P. Mangkorntong, N. Mangkorntong and S. Choopun, *Ceram. Int.*, 2008, 34, 823-826.
20 Y. H. Park, H. K. Song, C. S. Lee and J. G. Jee, *J. Ind. Eng. Chem.*, 2008, 14, 818-823.
21 M. S. Wu and H. W. Chang, *J. Phys. Chem. C*, 2013, **117**, 2590-2599.
22 F. Li, Y. Ding, P. Gao, X. Xin and Z. L. Wang, *Angew. Chem.*, 2004, 43, 5238-5242.
23 K. H. An, S. Y. Jeong, H. R. Hwang and Y. H. Lee, *Adv. Mater.*, 2004, 16, 1005-1009.
24 R. Yu, C. Pan, J. Chen, G. Zhu and Z. L. Wang, *Adv. Funct. Mater.*, DOI: 10.1002/adfm.201300593.
25 G. Zhu, A. C. Wang, Y. Liu, Y. Zhou and Z. L. Wang, *Nano Lett.*, 2012, 12(6), 3086-3090.
26 S. Xu, Y. Qin, C. Xu, Y. Wei, R. Yang and Z. L. Wang, *Nat. Nanotechnol.*, 2010, 5, 366-373.
27 Y. Qin, X. Wang and Z. L. Wang, *Nature*, 2008, 451, 809-813.
28 L. Gu, N. Y. Cui, L. Cheng, Q. Xu, S. Bai, M. M. Yuan, W. W. Wu, J. M. Liu, Y. Zhao, F. Ma, Y. Qin and Z. L. Wang, *Nano Lett.*, 2013, 13(1), 91-94.
29 N. Cui, W. Wu, Y. Zhao, S. Bai, L. Meng, Y. Qin and Z. L. Wang, *Nano Lett.*, 2012, 12, 3701-3705.
30 S. Bai, Q. Xu, L. Gu, F. Ma, Y. Qin and Z. L. Wang, *Nano Energ.*, 2012, 1, 789-795.
31 A. Janotti and C. G. Van de Walle, *Phys. Rev. B*, 2007, 76.
32 R. Yang, Y. Qin, L. Dai and Z. L. Wang, *Nat. nanotechnol.*, 2009, 4, 34-39.
33 Y. Hu, L. Lin, Y. Zhang and Z. L. Wang, *Adv. Mater.*, 2012, 24, 110-114.
34 Y. Zhang, Y. Liu and Z. L. Wang, *Adv. Mater.*, 2011, 23, 3004-3013.
35 F. Zhang, Y. Ding, Y. Zhang, X. Zhang and Z. L. Wang, *ACS Nano*, 2012, 6, 9229-9236.
36 D. Gu, S. K. Dey and P. Majhi, *Appl. Phys. Lett.*, 2006, 89, 082907.
37 S. Zhang, Y. Zhang, S. Huang, H. Liu, P. Wang and H. Tian, *The J. Phys. Chem. C*, 2010, 114, 19284-19288.
38 S. Ju, S. Kim, S. Mohammadi, D. B. Janes, Y.-G. Ha, A. Facchetti and T. J. Marks, *Appl. Phys. Lett.*, 2008, 92, 022104.
39 A. Kolmakov, D. Klenov, Y. Lilach, S. Stemmer and M. Moskovits, *Nano Lett.*, 2005, 5, 667-673.
40 S. Bai, L. Zhang, Q. Xu, Y. Zheng, Y. Qin and Z. L. Wang, *Nano Energy*, 2013, 2, 749-753.
41 R. Bajpai, A. Motayed, A. V. Davydov, V. P. Oleshko, G. S. Aluri, K. A. Bertness, M. V. Rao and M. E. Zaghloul, *Sensors Actuat. B-Chem.*, 2012, 171-172, 499-507.
42 M. Bowker and R. Madix, *Surf. Sci.*, 1982, 116, 549-572.

Table of contents entry:

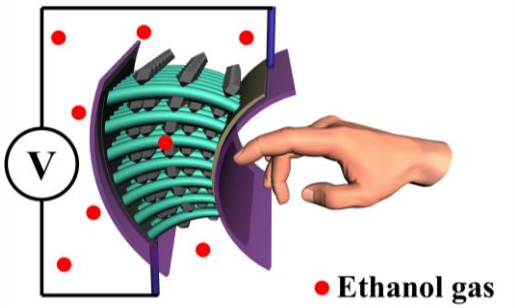

Room-temperature self-powered ethanol sensing has been realized from Pd/ZnO nanoarray nanogenerator under the driving of human finger movement